Investigation of Molar Concentration Effect on Structural and Optical Properties of Dip-Coated Copper Oxide Thin Films

Abul Monsur Mohammed Musa[a,b*], Md. Monuar Hossain[a]

[a]*Department of Civil Engineering, Uttara University, Dhaka-1230*
[b]*Department of Physics, Dhaka University of Engineering & Technology, Gazipur, 1707*

Abstract

This study aims to investigate the influence of molar concentration and film thickness on the structural and optical properties of dip-coated copper oxide (CuO) thin films. The dip-coating technique, maintaining a constant withdrawal speed is employed to synthesize CuO films with varying molar concentrations. The molar concentration determines the film's thickness. The structural, optical, and morphological properties are performed using X-ray diffraction (XRD) analysis, UV-Vis-NIR spectrophotometer, and scanning electron microscopy (SEM). The XRD analysis reveals that the molar concentration significantly impacts the structural properties, resulting in variations in the crystallinity and microstructural parameters of these films. The films exhibit varying optical absorbance, transmittance, and optical band gap depending on molar concentration. The SEM image of the films shows a porous, uniform surface morphology over a smooth background. The molar concentration along with film thickness plays a significant role in controlling the structural and optical properties of the dip-coated films, making them suitable for potential applications in optoelectronic devices and solar cell absorber layers.

Keywords: Dip-coating; Sol-gel; Molar concentration; Band gap.

1. Introduction

Copper oxide (CuO) thin films have attracted considerable attention in recent years due to their unique structural and optical properties, making them promising candidates for various applications in optoelectronic devices and solar cell absorber layers [1]. The advancement of p-type semiconductors holds great significance for device technologies based on solar cells, gas sensors, energy storage, and light-emitting diodes [2-4]. The special allure of CuO-based materials lies in their potential application in various optoelectronic devices. CuO has numerous advantages in catalysts and solar energy conversion applications due to the exceptional activity of oxidation and reduction reactions [3,4].

Copper oxide (CuO) is a promising metal oxide semiconductor with a monoclinic crystal structure, known for its low band gap, non-toxic nature, and high melting point. CuO thin film typically exhibits a transmittance of 20% in the long wavelength range of the visible region but this can reach up to 90% with a refractive index of 2 to 2.5 [1][4]. The band gap of CuO films varies from 1.2 to 2.1 eV depending on the deposition technique and film thickness [5]. The properties, both physical and chemical of these developed materials are often determined by the deposition methods involved. Various thin film deposition techniques have been utilized such as chemical bath deposition (CBD) [6], pulsed laser deposition (PLD) [7], electroplating [8], spray pyrolysis [9], and well-known sol-gel [1][4] techniques. Among other techniques, sol-gel dip-coating stands out due to its low cost, simplicity, high film-forming efficiency, and easy availability of equipment [5]. Musa et al [1] synthesized copper oxide (CuO) thin films on glass substrates by a facile sol-gel dip-coating technique with varying withdrawal speeds from 0.73 to 4.17 mm/s. The variation of film thickness manifested by dip-coating withdrawal speeds was investigated in detail for carbon dioxide (CO2) gas-sensing.

*Corresponding author:
E-mail address: monsur.civil@uttarauniversity.edu.bd

However, the study of the effect of the molar concentration of CuO thin film for optoelectronic application is rarely discussed. In this study, we aim to investigate the impact of molar concentration (MC) and film thickness on the structural and optical properties of dip-coated CuO thin films. Detailed studies of the fundamental characteristics of CuO based on MC have been limited for optoelectronic devices and solar cell applications. Therefore, the motivation of this research work is to synthesize a thickness-dependent CuO thin film by a cost-effective sol-gel dip-coating technique and also investigate the molar concentration effect of these deposited films.

2. Material and methods

2.1. Materials and preparation of CuO thin film

Prior the glass substrates having a dimension of 72.2 mm × 23.4 mm × 1.2 mm (Sail brand, China) were initially cleaned with detergent soap in clean water. Then the glass substrate was immersed in an ultrasonic bath containing specified chemicals for 20 minutes to eliminate impurities. After that acetone, ethanol, and deionized water were used for cleaning then argon gas was blown with the substrate for drying. Copper acetate monohydrate [Cu $(CH_3COO)_2$ H_2O] (MERCK, KGaA, 64271 Darmstadt, Germany (99.99% pure)) was utilized as precursor materials for CuO. Ethylene glycol [$C_6H_6O_2$], diethanolamine (DEA) [$C_4H_{11}NO_2$] (Germany), and isopropanol (IPA) [C_3H_7OH] were added as a coating material, stabilizer, and solvent respectively which were collected from the local market and manufactured by Worli, Mumbai, India.

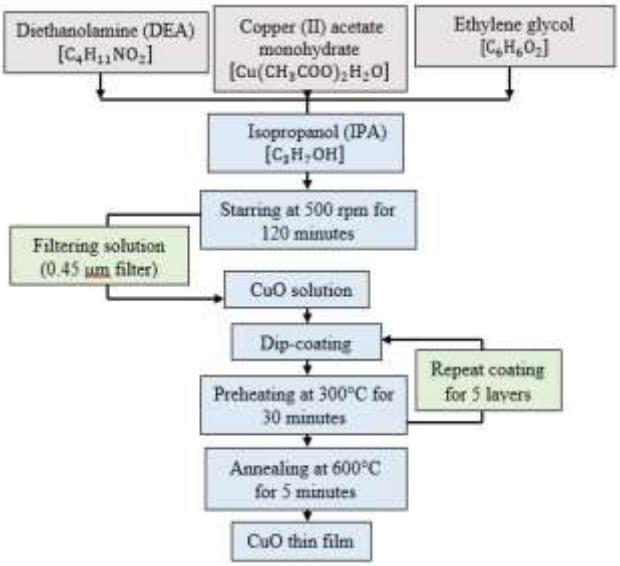

Fig. 1: Flowchart of synthesis technique of dip-coated CuO thin film.

The copper acetate powder was used to prepare 0.3 to 0.45 MC of precursor solution. It was found that, at lower precursor MCs (0.1–0.2) film surface was rough and not smooth, moreover, at higher MCs (0.4–0.45) the film surface was highly dense. For this reason, 0.25–0.35 MCs were selected for deposited CuO thin films. To synthesize MC's of 0.25, 0.3, and 0.35, the precursor materials were dissolved with Isopropanol (9 ml) and diethanolamine (0.5 ml), then ethylene glycol (0.5 ml) which were added to a 10 ml solution. A magnetic stirrer was used to stir the solution at a speed of 300 rpm for 2 hours, resulting in a final solution that had a bluish-dark and clean color. A 0.45 μm filter was employed for filtering the solution. Next, the glass substrate was dipped in the solution at a constant withdrawal speed of 4.5 mm/s. After each dipping of the glass substrate, the film was dried for 30 minutes in a drier (furnace) at a temperature of 300 °C. To achieve a higher thickness with recrystallization, this process was repeated five times. Subsequently, the film was annealed at a temperature of 600°C for 5 minutes.

2.2 Materials characterization

The X-ray diffraction (XRD) technique (Bruker D8 Advance Diffractometer (Germany)) with a Cu–Kα radiation, out of plane geometry at 1.5406 Å and functioning at 40 kV and 30 mA, was utilized for analyzing the crystallite structure of CuO films. The range of scattering angle of XRD was 30°–80°. The vibrational structure from 100–700 cm^{-1} was recorded using the Macro Raman HORIBA (Japan).

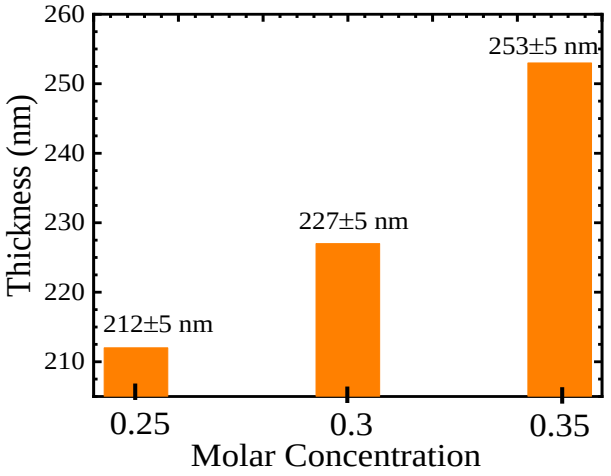

Fig. 2: Thickness versus MCs of deposited dip-coated CuO thin films.

The Raman laser excitation wavelength was 785 nm with laser strength (≤ 5 mW). A UV-vis-NIR spectrophotometer (SHIMADZU-2600, Japan) was utilized to determine the optical characteristics of the films. An Alpha-Step D-500, KLA, USA was used for measuring the thickness of CuO thin films with three times scan. Using a scanning electron microscope (SEM, ZEISS EVO18), the surface morphology of the CuO films was determined.

3. Results and discussion

3.1 Structural analysis

3.1.1 XRD diffraction analyses

The X-ray diffraction (XRD) patterns displayed in Figure 3 compare the thin films that were synthesized using various MCs. In these patterns, the CuO films exhibit distinct diffraction peaks at specific 2θ values: 32.52, 35.58, 38.7, 48.84, 53.48, 58.24, 61.7, 70.1, 73.3 and 77.8. These peaks correspond respectively to the (110), $(\bar{1}11)$, (111), $(\bar{2}02)$, (020), (202), $(\bar{1}13)$, $(\bar{3}11)$, (220), and (311) planes of the monoclinic CuO phase, as identified by the JCPDS card no. 48-1548 [6]. The presence of these diffraction peaks indicates that the CuO films possess a polycrystalline structure [10]. Notably, the most prominent peaks at 32.52° and 35.58° can be attributed to the $(\bar{1}11)$ and (111) planes, respectively. Importantly, no Bragg's peaks associated with Cu_2O or metallic Cu phase are observed in the XRD patterns, suggesting that the MC-based thin films predominantly consist of pure CuO [7]. To further validate the phase purity, Raman spectra were recorded and are presented in Figure 4.

The important microstructural parameters, including the size of crystallites (d), dislocation density (δ), microstrain (ε), and X-ray density (ρ) were computed using the following equations [8].

$$d = \frac{k\lambda}{\beta cos\theta} \quad (1)$$

$$\varepsilon = \frac{\beta cos\theta}{4} \quad (2)$$

$$\delta = \frac{1}{d^2} \quad (3)$$

$$\rho = \frac{nM_w}{NV} \quad (4)$$

The constant k is determined by the shape factor of the crystallite or grain and has a value of 0.94 for spherical crystallites or grains. In the provided equations, λ represents the X-ray wavelength, t is the film thickness, β corresponds to the full with at half maximum (FWHM) in degrees, which is adjusted for instrumental broadening by fitting the peaks with an XRD tool. Lastly, θ denotes the Bragg angle associated with the $\{h\ k\ l\}$ reflection. The number of atoms and the volume of the unit cell is n and V, Mw is the molecular weight, and N is Avogadro's number.

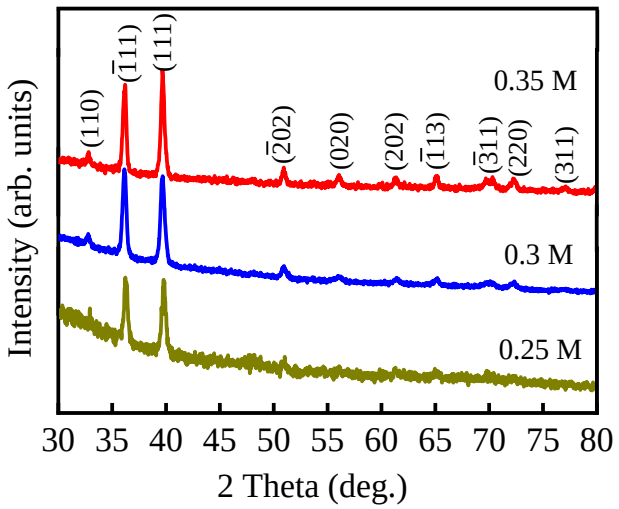

Fig. 3: XRD patterns of CuO films of different thicknesses with precursor MCs of 0.25, 0.3, and 0.35.

Table 1: Microstructural parameters including crystallite size (d), dislocation density (δ), microstrain (ε), and X-ray density (ρ) associated with $(\bar{1}11)$ diffraction plane with MCs of dip-coated CuO films.

MC	t (nm) ± 5	2θ (deg.)	d (nm) ±0.01	δ (10^{-4}/nm^2)	$\varepsilon \times$ (10^{-4})	ρ (g/cm^3)
0.25	212	35.58	21.23	4.8	5.7	3.47
0.3	227	35.52	31.27	11.9	7.3	4.13
0.35	253	35.54	39.12	15.6	11.7	6.15

It has been noted that as the film thickness increases with the MCs from 212 ± 5 to 253 ± 5 nm, the crystallite size increases from 21.23 ± 0.01 to 39.12 ± 0.01 nm. The films with greater thickness (0.35 MC) exhibit larger crystallite size, indicating reduce dislocation densities and strain [9]. This consistent trend suggests an enhancement in the crystallinity of the film and a reduction in lattice imperfections as the film thickness increase. The decrease in crystal strain indicates a relaxation stress in the thicker CuO films obtained through dip-coating [11].

The X-ray density is influenced by the extent of X-ray beam absorption within the sample. A denser film exhibits greater absorption of the X-ray beam in contrast to structures with lower density. In the film deposited with higher MC, there is a higher absorbed species on the substrate surface found compared with lower MC films. During annealing, thicker films tend to exhibit more porosity than thinner ones, as lower MC results in thinner films with comparatively lower solvent impregnation [12]. The effect can be observed through the SEM surface and optical analyses discussed in the next sections.

3.1.2 Raman analyses

In Figure 4, a comparison is made between dip-coated thin films that were prepared with different MCs. The significant phonon modes observed in the CuO phase are approximately ~296 cm^{-1} (Ag), ~346 cm^{-1} ($Bg^{(1)}$), and ~630 cm^{-1} ($Bg^{(2)}$) [13][14]. For Cu_2O phase, the prominent modes are around ~150 cm^{-1}($T1u^{(1)}$), ~220 cm^{-1} (2Eu), ~304 cm^{-1} (A2u), ~520 cm^{-1} (T2g) ~615 cm^{-1} ($T1u^{(2)}$) [15]. These Raman peaks of the dip-coated thin films strongly align with the monoclinic CuO phase and indicate the absence of other CuO phases, which supports the findings from XRD analysis. The intensity of the main Raman peak Ag in dip-coated CuO films at 0.35 MC is noticeably higher compared to other films, suggesting improved crystallinity and the highest thickness among all studied films [16]. This observation is consistent with the measured film thickness presented in Figure 1.

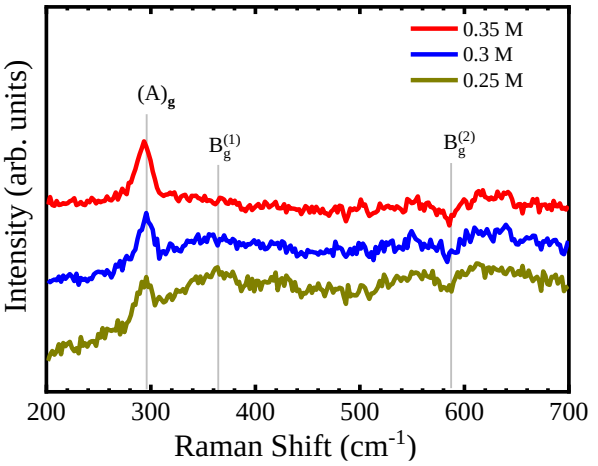

Fig. 4: Raman spectra of CuO films of different thicknesses prepared with precursor MCs of 0.35, 0.3, and 0.25.

3.2 Morphological analyses

Figures 5(a) and 5(b) show the SEM micrographs of CuO thin films using MCs of 0.25 and 0.35. The film grown with 0.35 MC exhibits the most porous microstructure compared to the other film. As the MC decreases, the porous nature of the films appears to diminish [17]. The presence of numerous pores on the film surface enhances the accessibility of the sensing gas of the film, thereby increasing the available active area of the gas absorption [18].

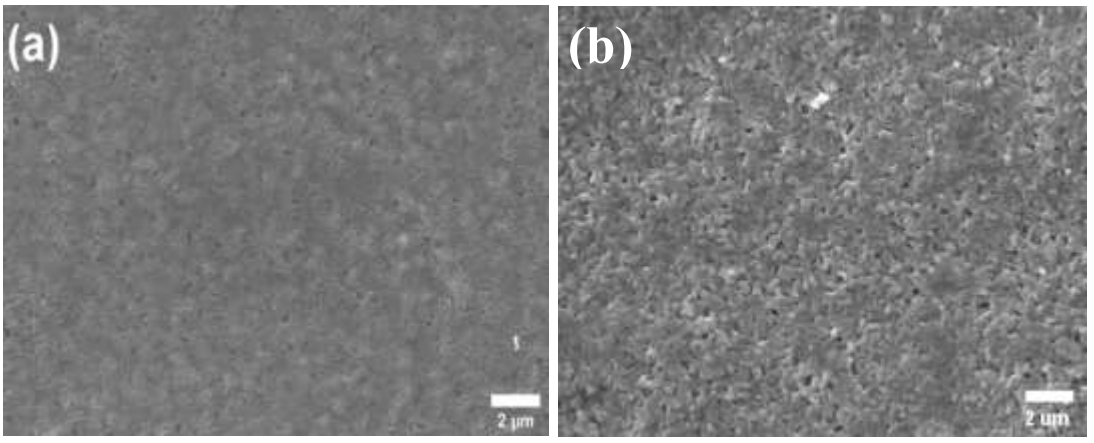

Fig. 5: SEM micrograph of representative CuO dip-coated films grown on a glass substrate of (a) 0.25 and (b) 0.35 MC with ×15k magnification.

The determined grain sizes are 138 ± 5 and 163 ± 5 nm for the sample deposited to 0.25 and 0.35 MC respectively, which are found using ImajeJ 2020 latest version software by considering ten grain for the average grain size of the sample. The observation of grain size variation is related to the estimated crystallite size from XRD analyses. Thicker films exhibit larger grains, which can contribute to the porous nature of the deposited film during the thermal treatment process [15], allowing the organic solvent within the film.

3.3 Optical Properties

Figure 6(a) shows the optical absorbance (*A*) of the deposited films at various MC's.

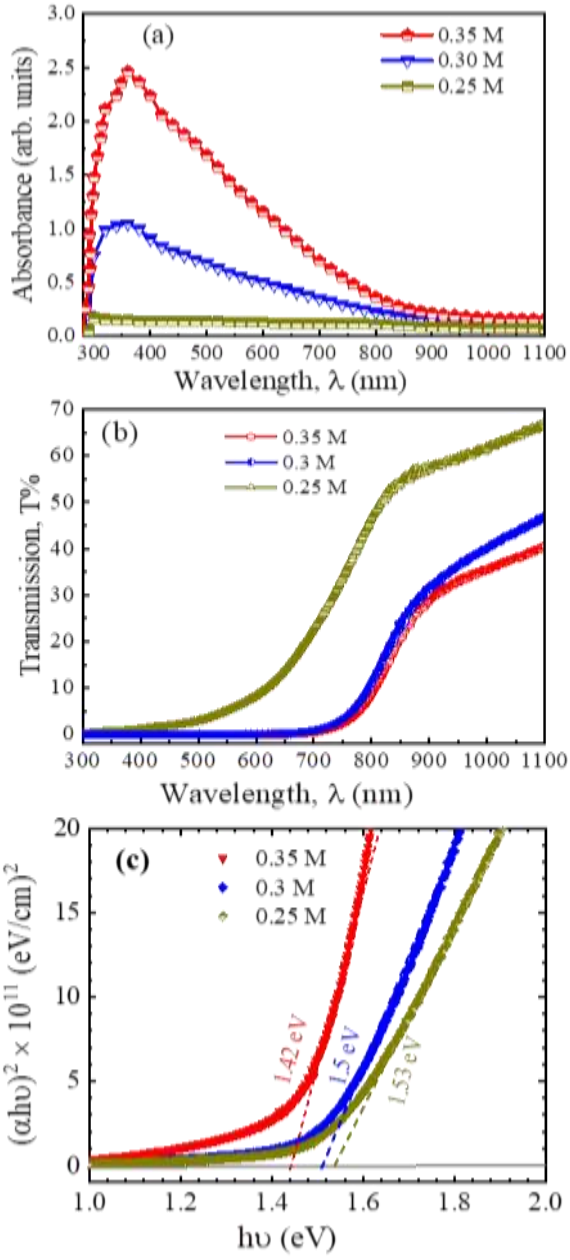

Fig. 6: (a) Optical absorbance, (b) transmittance, and (c) the plots of $(\alpha h\upsilon)^2$ versus $h\upsilon$ of dip-coated CuO films of different thicknesses prepared with precursor MCs of 0.35, 0.3, and 0.25.

These absorbance spectra demonstrate that all the films exhibit high absorbance in the visible region, which is a characteristic feature of CuO films suitable for use as absorber layers in solar cell applications [19]. It is evident that, *A* exhibits a sharp increase in the ultraviolet (UV) region, reaches a maximum value in the visible region, and then remains constant in the near-infrared (NIR) region (800-1100 nm) [20]. The highest value of *A* observed at 360 nm for 0.35 MC. The intensity of the spectra increases with an increase in MC as well as the value of *t*. These phenomena can be attributed to the fact that higher concentrations result in more CuO crystals absorbing the photon energy. The optical absorption at the absorption edge is associated with the transition from the valance band to the conduction band and is indicative of the band gap energy being closed [21]. The optical properties of CuO thin films were investigated by studying their optical transmission (*T*) at different MCs. It is observed that the transmission of the films decreased from 55 to 15% in the 850 nm region as the film thickness increased (refer to Fig. 6(b)).

The value of *T* increased significantly with longer wavelengths in the visible region and showed transparency in the NIR region of spectra [22]. Furthermore, the decrease in optical transmittance with MCs can be attributed to the increasing film thicknesses [21] as seen in Fig. 6(b). The Tauc plot, generated using the optical transmission data from Figure 6(c), was used to estimate the values of E_g. These values are obtained by extrapolating the linear portion of $(\alpha hv)^2$ to the X-axis. A band gap denotes the separation between the valence band and the conduction band, defining the minimum energy necessary to elevate an electron to a state within the conduction band, enabling its involvement in conduction. The optical band gap of the dip-coated films is determined to be 1.42, 1.5, and 1.53 eV for MCs of 0.35, 0.3, and 0.25 respectively. These values closely match the reported optical band gap of CuO thin films in the literature [23]. Note that, the band gap energy decreases with increasing film thickness due to the growth of crystallite size.

The increase in film thickness may lead to the narrowing of the optical band gap. This phenomenon can be attributed to either a higher disorder of phonon states or higher carrier concentration in the dip-coated CuO thin film [24]. Furthermore, high absorbance, as well as low transmittance and the porous structure, are found in these thickness-dependent deposited films. It is seen that tailorable physical properties offer notable potential for solar cell and optoelectronic device applications [25].

Conclusion

A detailed investigation is conducted for the influence of precursor MCs as well as the film thickness of dip-coated CuO thin films. The structural, morphological, and optical properties of these films have been recorded. XRD analysis revealed that the films exhibited a polycrystalline nature, monoclinic CuO crystal structure with preferential orientations along the (111) and $(\bar{1}11)$ planes. No impurity phase is found, further confirmed by Raman analysis. The size of crystallinity in the deposited films increased from 21.23 to 39.12 nm with the increase in film thickness. The larger porosity is observed for high thickness. The optical direct band gap decreases from 1.42 to 1.53 eV with the increase in MC as well as thickness, which can be attributed to the increase in carrier concentration. A significant improvement in optical properties is observed due to the increase of MC. High absorbance, low transmittance, smooth porous structure, and lower optical band gap indicate that the synthesized films are appropriate for solar cell absorber layer and optoelectronic devices applications.

Author contributions

A.M.M. Musa: Investigation, Conceptualization, Formal analysis, Methodology, Visualization, Resources, Validation, Project administration, Funding acquisition, Writing - original draft, review & editing. **M.M. Hossain:** Formal Analysis, and Review.

Acknowledgments

The authors would like to concede the help of the Center for Research and Training (CRT) of Uttara University, Uttara, Dhaka-1230 for the financial support (Grant: P-10/CIE-6/CRT 2023) for this research, and Bangladesh Council of Scientific and Industrial Research (BCSIR), Dhaka-1205, for providing the laboratory facilities.

Conflict of Interest

The authors declared that they have no conflict of interest.

References:

[1] Musa, A.M.M., Farhad, S.F.U., Gafur, M.A. and Jamil, A.T.M.K., 2021. Effects of withdrawal speed on the structural, morphological, electrical, and optical properties of CuO thin films synthesized by dip-coating for CO2 gas sensing. *AIP Advances*, *11*(11).

[2] Mårtensson, N., 2011. Optical properties of silica-copper oxide thin films prepared by spin coating.

[3] Rydosz, A., 2018. The use of copper oxide thin films in gas-sensing applications. *Coatings*, *8*(12), p.425.

[4] Tanvir, N.B., Yurchenko, O., Wilbertz, C. and Urban, G., 2016. Investigation of CO 2 reaction with copper oxide nanoparticles for room temperature gas sensing. *Journal of materials chemistry A*, *4*(14), pp.5294-5302.

[5] Dolai, S., Dey, R., Das, S., Hussain, S., Bhar, R. and Pal, A.K., 2017. Cupric oxide (CuO) thin films prepared by reactive dc magnetron sputtering technique for photovoltaic application. *Journal of Alloys and Compounds*, *724*, pp.456-464.

[6] Samarasekara, P., Kumara, N.T.R.N. and Yapa, N.U.S., 2006. Sputtered copper oxide (CuO) thin films for gas sensor devices. *Journal of Physics: Condensed Matter*, *18*(8), p.2417.

[7] Murali, D.S., Kumar, S., Choudhary, R.J., Wadikar, A.D., Jain, M.K. and Subrahmanyam, A., 2015. Synthesis of Cu2O from CuO thin films: Optical and electrical properties. *AIP advances*, *5*(4).

[8] Moumen, A., Hartiti, B., Thevenin, P. and Siadat, M., 2017. Synthesis and characterization of CuO thin films grown by chemical spray pyrolysis. *Optical and Quantum Electronics*, *49*, pp.1-12.

[9] Das, H.T., Vinoth, S., Thirumoorthi, M., Alshahrani, T., Hegazy, H.H., Somaily, H.H., Shkir, M. and AIFaify, S., 2021. Tuning the optical, electrical, and optoelectronic properties of CuO thin films fabricated by facile SILAR dip-coating technique for photosensing applications. *Journal of Inorganic and Organometallic Polymers and Materials*, *31*, pp.2606-2614.

[10] Wu, W., Brongersma, S.H., Van Hove, M. and Maex, K., 2004. Influence of surface and grain-boundary scattering on the resistivity of copper in reduced dimensions. *Applied physics letters*, *84*(15), pp.2838-2840.

[11] Liang, J., Kishi, N., Soga, T., Jimbo, T. and Ahmed, M., 2012. Thin cuprous oxide films prepared by thermal oxidation of copper foils with water vapor. *Thin Solid Films*, *520*(7), pp.2679-2682.

[12] Sonia, S., Kumar, P.S., Jayram, N.D., Masuda, Y., Mangalaraj, D. and Lee, C., 2016. Superhydrophobic and H 2 S gas sensing properties of CuO nanostructured thin films through a successive ionic layered adsorption reaction process. *RSC advances*, *6*(29), pp.24290-24298.

[13] Saadaldin, N., Alsloum, M.N. and Hussain, N., 2015. Preparing of copper oxides thin films by chemical bath deposition (CBD) for using in environmental application. *Energy procedia*, *74*, pp.1459-1465.

[14] Farhad, S.F.U., Webster, R.F. and Cherns, D., 2018. Electron microscopy and diffraction studies of pulsed laser deposited cuprous oxide thin films grown at low substrate temperatures. *Materialia*, *3*, pp.230-238.

[15] Mali, S.M., Narwade, S.S., Navale, Y.H., Patil, V.B. and Sathe, B.R., 2019. Facile synthesis of highly porous CuO nanoplates (NPs) for ultrasensitive and highly selective nitrogen dioxide/nitrite sensing. *RSC advances*, *9*(10), pp.5742-5747.16.

[16] De, S., Higgins, T.M., Lyons, P.E., Doherty, E.M., Nirmalraj, P.N., Blau, W.J., Boland, J.J. and Coleman, J.N., 2009. Silver nanowire networks as flexible, transparent, conducting films: extremely high DC to optical conductivity ratios. *ACS nano*, *3*(7), pp.1767-1774.

[17] Farhad, S.F.U., Hossain, M.A., Tanvir, N.I., Akter, R., Patwary, M.A.M., Shahjahan, M. and Rahman, M.A., 2019. Structural, optical, electrical, and photoelectrochemical properties of cuprous oxide thin films grown by modified SILAR method. *Materials Science in Semiconductor Processing*, *95*, pp.68-75.

[18] Qasrawi, A.F. and Hamamdah, A.A., 2020. Thickness effects on the dielectric dispersion and optical conductivity parameters of CuO thin films. *Microwave and Optical Technology Letters*, *62*(4), pp.1453-1458.

[19] Ravichandiran, C., Sakthivelu, A., Davidprabu, R., Valanarasu, S., Kathalingam, A., Ganesh, V., Shkir, M., Algarni, H. and AlFaify, S., 2019. In-depth study on structural, optical, photoluminescence and electrical properties of electrodeposited Cu2O thin films for optoelectronics: An effect of solution pH. *Microelectronic Engineering*, *210*, pp.27-34.

[20] Qiu, G., Dharmarathna, S., Zhang, Y., Opembe, N., Huang, H. and Suib, S.L., 2012. Facile microwave-assisted hydrothermal synthesis of CuO nanomaterials and their catalytic and electrochemical properties. *The Journal of Physical Chemistry C*, *116*(1), pp.468-477.

[21] Shrividhya, T., Ravi, G., Hayakawa, Y. and Mahalingam, T., 2014. Determination of structural and optical parameters of CuO thin films prepared by double dip technique. *Journal of Materials Science: Materials in Electronics*, *25*, pp.3885-3894.

[22] Naveena, D., Logu, T., Dhanabal, R., Sethuraman, K. and Bose, A.C., 2019. Comparative study of effective photoabsorber CuO thin films prepared via different precursors using chemical spray pyrolysis for solar cell application. *Journal of Materials Science: Materials in Electronics*, *30*, pp.561-572.

[23] Tombak, A., Benhaliliba, M., Ocak, Y.S. and Kiliçoglu, T., 2015. The novel transparent sputtered p-type CuO thin films and Ag/p-CuO/n-Si Schottky diode applications. *Results in Physics*, *5*, pp.314-321.

[24] Daira, R., Kabir, A., Boudjema, B. and Sedrati, C., 2020. Structural and optical transmittance analysis of CuO thin films deposited by the spray pyrolysis method. *Solid State Sciences*, *104*, p.106254.

[25] Djebian, R., Boudjema, B., Kabir, A. and Sedrati, C., 2020. Physical characterization of CuO thin films obtained by thermal oxidation of vacuum evaporated Cu. *Solid State Sciences*, *101*, p.106147.